EVALUATION OF SAFETY DISTANCES RELATED TO UNCONFINED HYDROGEN EXPLOSIONS

Dorofeev, S.B.
FM Global, 1151 Boston-Providence Turnpike, Norwood, MA 02062, USA

ABSTRACT

A simple approximate method for evaluation of blast effects and safety distances for unconfined hydrogen explosions is presented. The method includes models for flame speeds, hydrogen distribution, blast parameters, and blast damage criteria. An example of the application of this methodology for hydrogen releases in three hypothetical obstructed areas with different levels of congestion is presented. The severity of the blast effect of unconfined hydrogen explosions is shown to depend strongly on the level of congestion for relatively small releases. Extremely large releases of hydrogen are predicted to be less sensitive to the congestion level.

1. INTRODUCTION

Hydrogen releases that can be expected in various accidents can result in formation of combustible mixtures of hydrogen with air. It has been shown by many investigators that weak ignition in these mixtures can easily result in efficient Flame Acceleration (FA), development of fast combustion regimes, and, under certain conditions, in the transition from deflagration to detonation. Pressure effects associated with fast combustion regimes can be very severe. This suggests that it is important to pay a special attention to explosion effects related to potential hydrogen releases.

It is generally agreed that hydrogen releases in confined and semi-confined geometries (tunnels, parking, garages, etc.) represent a significant safety problem, because of the principal possibility of hydrogen accumulation, and because of the promoting role of confinement for FA and pressure build-up. Unconfined hydrogen explosions can also represent a significant safety concern in situations where hydrogen releases take place in obstructed areas (refuelling stations, hydrogen production units, etc.). In these cases, relatively fast dilution of hydrogen-air mixtures at open air and inefficiency of FA without confinement can principally reduce possible consequences of the explosions. On the other hand, these effects can be easily overbalanced by relatively large quantities of hydrogen released.

Potential consequences of unconfined hydrogen explosions are the factors that should determine safety distances for various units of hydrogen infrastructure, which deal with significant quantities of hydrogen. The major consequences of unconfined explosions are connected with blast effects, thermal effects and effects of explosion-generated fragments. Although thermal and fragment effects may be of considerable importance in some cases, the blast effects of explosions are usually of the prime interest for determination of the safety distances. This may be especially important for hydrogen because of potentially severe blast effects. Unconfined hydrogen explosions and their blast effects are the focus of the present study.

A detailed analysis of the blast effects of accidental explosions of hydrogen should generally include studies of hydrogen release and distribution; an analysis of flame propagation, pressure build-up and blast generation in complex three-dimensional (3D) geometry; a study of the blast wave propagation and its effect on the surrounding objects. Because of the nature of the problems involved, this would generally require an application of 3D computer fluid dynamics simulations, which would be difficult or impossible to apply for all variety of the cases / applications. A simple approximate analytical tool should be useful in most cases. It can be also applied as a screening tool to select the cases where the detailed analysis may be necessary.

1

The objective of this study is to develop a simple approximate method for evaluation of blast effects and safety distances for unconfined hydrogen explosions. The proposed method includes:
(i) a model for evaluation of hydrogen flame speeds in obstructed areas;
(ii) a model for properties of "worst case" hydrogen distribution;
(iii) a model for blast parameters;
(iv) a set of blast damage criteria.

The following presentation includes a description of the method and an example of its application for hydrogen releases in three hypothetical obstructed areas with different levels of congestion.

2. METHODOLOGY

2.1 Evaluation of flame speeds in obstructed areas

It is well known (see, e.g., [1, 2]) that the amplitude of the pressure waves generated by gaseous explosions essentially depends on the maximum flame speed achieved during the combustion process. It is therefore important to have a reliable estimate for the flame speed as a function of the propagation distance and obstacle geometry.

In the following model an initially spherical flame is considered, which propagates from an ignition source through an obstructed area. The flame speed relative to a fixed observer at a distance R from ignition, V_f, depends on the burning velocity (generally turbulent), S_T, flame area, A_f, and on the ratio of densities between the reactants and products, σ:

$$V_f = \sigma S_T \frac{A_f}{A_R} \; ,$$
(1)

where $A_R = 4\pi R^2$ is the area of the spherical flame at R.

The flame speed increases due to the increase of the flame area (flame folding) in an obstacle field and due to the increase of the turbulent burning rate during flame propagation. The latter effect should also describe the increase of the flame speed with distance in a system without obstacles.

The flame folding effect can be approximately described applying simple geometrical considerations as it was suggested in [3, 4]. If one considers a uniform obstacle field with distance between obstacles, x, and their characteristic size, y, the following assumptions can be made. The flame is considered to be folded due to interactions of the flame with obstacles and forms a flame brush. Each obstacle inside the brush contributes the value of $4xy$ to the total flame surface. Up to a certain distance from the ignition point, R_0, the flame brush width is equal to the flame of radius R. This yields:

$$\frac{A_f}{A_R} = 1 + \frac{4}{3} \frac{yR}{x^2} \; .$$
(2)

Flame propagation at $R > R_0$ results in a situation where the flame brush width is smaller than the flame radius R. The width of the brush can be estimated as σx because the flame tips extend with velocity σS_T in the direction of the flame propagation and disappear at the rear of the brush, because of burning with the velocity S_T in the perpendicular direction. Thus at some $R \gg R_0$, one should expect:

$$\frac{A_f}{A_R} = 1 + \frac{4\sigma y}{x} \; .$$
(3)

2

If one assumes that Eq. (2) is valid for $R = R_0 = \sigma x$, Eq. (3) is valid at $R = n\sigma x$, where $n \gg 1$, and that the increase in the flame area with distance can be described with a power law:

$$\frac{A_f}{A_R} = 1 + AR^\alpha \ ,$$

(4)

then the parameters of equation (4) can be expressed as:

$$A = \frac{4}{3} \frac{\sigma y}{x(\sigma x)^\alpha} \ ,$$

(5)

$$\alpha = \log_n 3 \ .$$

(6)

Exponent α may be considered as an unknown parameter of the order of 0.5 (for example, $\alpha \approx 0.48$ for $n = 10$) and Eq. (1) becomes:

$$V_f = \sigma S_T \left(1 + \frac{4}{3} \frac{\sigma y}{x} \frac{R^\alpha}{(\sigma x)^\alpha} \right) .$$

(7)

Effect of turbulence can be accounted for by applying Bradley correlation [5] for turbulent burning velocity, S_T:

$$\frac{S_T}{S_L} = a \left(\frac{u'}{S_T} \right)^{1/2} \left(\frac{L_T}{\delta} \right)^{1/6} ,$$

(8)

where u' is turbulent fluctuation velocity; S_L – laminar burning velocity; L_T – integral length scale of turbulence; $\delta = \nu/S_L$ is the laminar flame thickness; ν – viscous diffusivity; and a is a coefficient. Turbulent fluctuation velocity, u', can be considered as a small portion of the flow speed, V, ahead of the flame:

$$u' = bV = bV_f \frac{\sigma - 1}{\sigma} \ ,$$

(9)

where b is a coefficient of the order of 10^{-2}. Equations (7-9) yield:

$$V_f = a^2 b \sigma (\sigma - 1) S_L \left(1 + \frac{4}{3} \frac{\sigma y}{x} \frac{R^\alpha}{(\sigma x)^\alpha} \right)^2 \left(\frac{L_T}{\delta} \right)^{1/3} .$$

(10)

Equation (10) gives an approximate description of the flame speed as a function of distance in an area with or without obstacles. It is seen that a significant increase of the flame speed with distance can be only expected in a system with obstacles, $y \neq 0$. In this case the contribution of parameter (L_T/δ) is relatively weak. In the case of no obstacles, $y = 0$, the only value to estimate L_T is the flame radius, and the flame speed increases as $R^{1/3}$, which should be considered as a reasonable outcome for spherical flames without obstacles. Mixture properties are accounted for in Eq. (10) through the values of the laminar burning velocity, S_L, and expansion ratio, σ.

An application of the correlation (10) for the flame speed requires determination of two unknown parameters $a^2 b$ and α. For the purposes of the present analysis, these parameters were evaluated using experimental data on the flame speeds as a function of distance inside obstacle arrays [4, 6] and data on flames with no obstacles [7, 8]. Data for relatively high reactive fuels, including hydrogen, ethylene

and propylene were selected for a wide range of distances and flame speeds (see Fig. 1). Parameters a^2b and α were determined from fitting of experimental data with function (10) using the least squares method. The results of the fitting procedure are presented in Fig. 2.
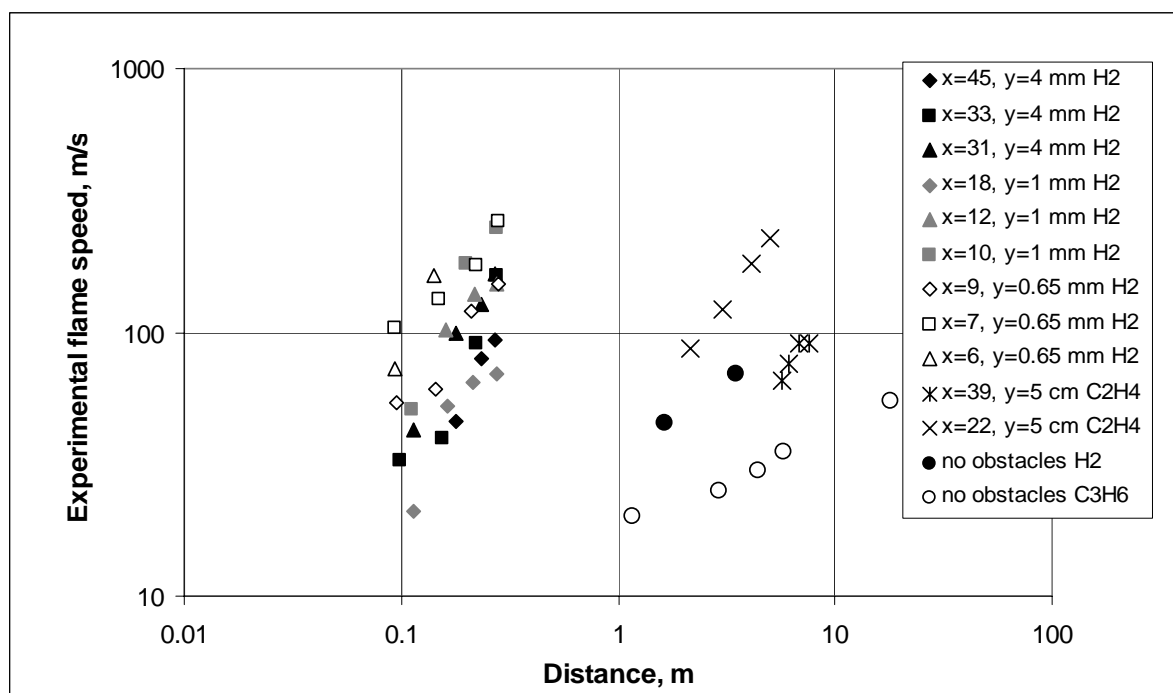

Figure 1. Range of experimental data on flame speed vs distance used in flame speed correlation.
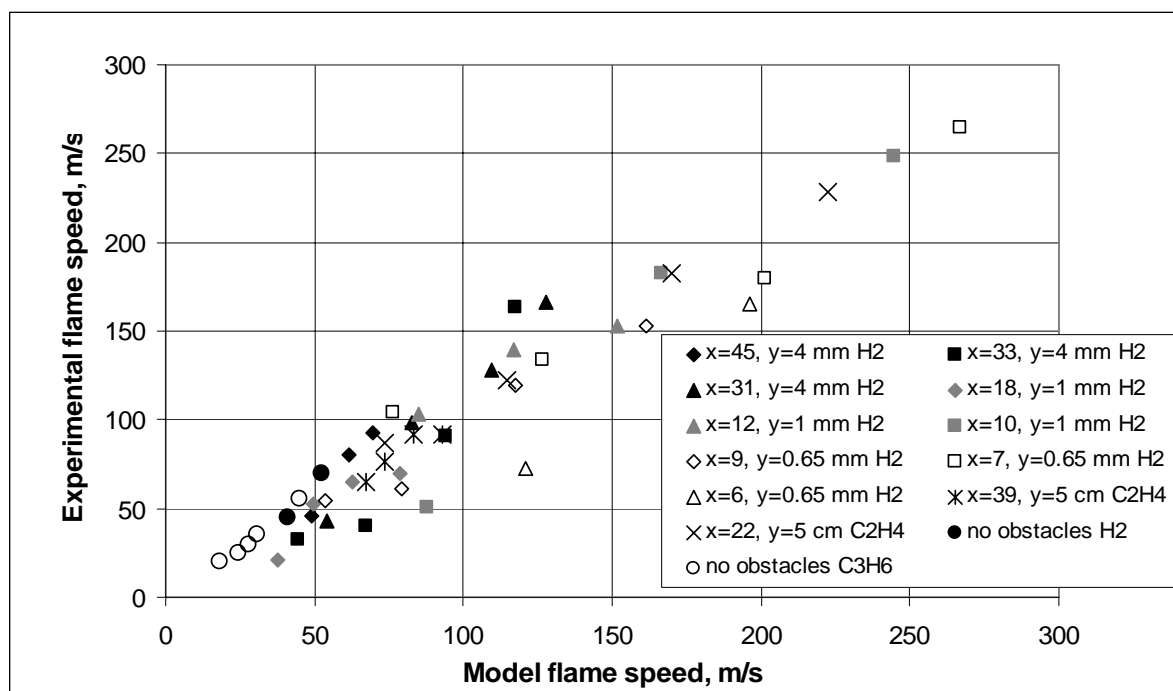

Figure 2. Comparison of flame speed correlation (a^2b = 8.5e-3, α = 0.63) with experimental data.

4

The model for the flame speed presented here appeared to be in a good agreement with the results of large-scale experimental data [9], presented recently in [10]. The flame speeds of about 40 and 80 m/s are reported in [10] for unconfined deflagrations in 29.7 vol. % of hydrogen in air at distances of 3 and 14 m from ignition correspondingly. Equation (10) gives 50 and 84 m/s for these distances (3 and 14 m), which is in agreement with the experimental data within the limits of accuracy of the model.

2.2 Hydrogen distribution

The amplitudes of the pressure waves generated by hydrogen explosions are expected to depend on the concentration distribution of hydrogen in air resulted from its release. The pressure waves generally become stronger with increase of the total energy of combustion. The blast effect also becomes more severe with the increase of the flame speed.

In the present section the focus is on determination of the conservative case of hydrogen distribution for fast or nearly instantaneous releases of hydrogen. We do not consider relatively slow hydrogen releases here, which are not capable of creating a combustible mixture under unconfined conditions. The assumption that all the released hydrogen forms a stoichiometric mixture with air is not used here as a conservative, or "worst case". Such a situation is considered here to be practically impossible as a result of an unconfined accidental release of hydrogen.

There is clearly a variety of release scenarios, which can affect the resulting hydrogen distribution. Instead of considering specific scenarios here, a simple general model will be analysed. This approximate general model assumes that the released hydrogen forms a cloud with a non-uniform hydrogen concentration. The form of the cloud is assumed to be semi-spherical, for simplicity. Hydrogen concentration is considered to reach the maximum in the centre of the semi-sphere and decreases linearly with radius. Linear decrease of the concentration with radius is chosen for simplicity as well.

The postulated properties of the hydrogen distribution are used here only for the purpose to limit the number of parameters that determine average cloud properties, and, thus, to be able to select the "worst case". With the above assumptions, properties of hydrogen cloud is fully defined by two parameters: the maximum hydrogen concentrations, C_{max}, in the cloud centre, and the total hydrogen mass in the cloud, m. Once the "worst case" is selected, only average cloud properties will be used to evaluate the explosion effect, making the assumed details of the hydrogen distribution relatively unimportant at that stage.

One can define the following properties of the hydrogen distribution, which affect the severity of the blast effect. These are the total combustion energy released, E; average laminar flame speed, $<S_L>$; average expansion ratio, $<\sigma>$; and average value, $<\gamma>$, of term $\gamma = \sigma(\sigma-1)S_L$, which defines the flame speed according to Eq. (10). A comparison of these properties calculated as functions of the maximum hydrogen concentrations, C_{max}, for the same total hydrogen mass is presented in Fig. 3.

The average values of the properties were defined using integration over the volume of flammable cloud, W. This is illustrated by the following equation for $<S_L>$:

$$< S_L >= \frac{1}{W} \int_W S_L(C) \cdot 2\pi r^2 dr \ , \tag{11}$$

where $C = C(r)$ – hydrogen concentration, r – radius from cloud centre.

Figure 3 shows that the total energy reaches maximum at $C_{max} \approx 50\%$ vol., while the value of $<\gamma>$ at $C_{max} \approx 88\%$ vol. It is reasonable to assume that the "worst case" is close to the case where $<\gamma>$ reaches maximum ($C_{max} \approx 88\%$ vol.), because the variation of E is relatively small compared to that of $<\gamma>$. Also, the blast effect can be shown (see section 2.3) to be determined by $<\gamma>^2$ and $E^{1/3}$ as parameters.

The average properties of this "worst case" are given by: $\langle S_L \rangle$ = 1.4 m/s; $\langle \sigma \rangle$ = 3.75; and explosion energy, E, is 0.6 of the total chemical energy of hydrogen in the cloud.

The estimated value for the energy, E, does not mean that the explosion effect would be equivalent to that of an ideal (TNT) explosion with the energy of 60% of the total chemical energy of hydrogen released. This would be extremely conservative assumption. We should emphasise that in the model presented here the explosion effect is a function of the flame speed, which is proportional to parameter γ, which, in its turn, is estimated to be only of about 0.1 of its maximum value for our "worst case".
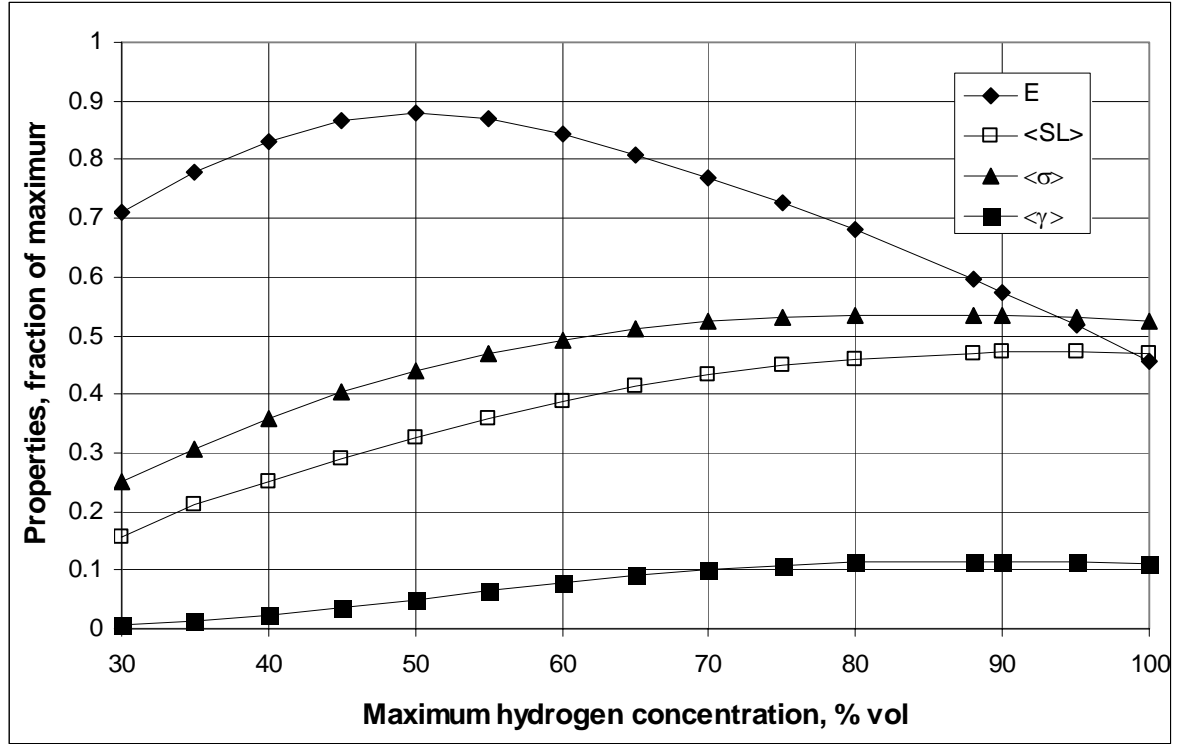

Figure 3. Average properties of hydrogen clouds, E, $\langle S_L \rangle$, $\langle \sigma \rangle$, and $\langle \gamma \rangle$ presented as fractions of their maximum achievable values versus maximum hydrogen concentration in the clouds.

2.3 Blast parameters

Calculations of blast parameters are based on the methodology presented in [2]. Maximum blast overpressure, P, and positive impulse, I, are calculated as a function of distance, R, from the blast epicenter using dimensionless Sach's variables for distance, R^*, overpressure, P^* and impulse, I^*:

$$R^* = \frac{R p_0^{1/3}}{E^{1/3}} \, , \tag{12}$$

$$P^* = P / p_0 \, , \tag{13}$$

$$I^* = \frac{I a_0}{E^{1/3} p_0^{2/3}} \, , \tag{14}$$

where p_0 and a_0 are pressure and sound speed in the surrounding air.

According to [2], dimensionless overpressure and impulse are considered to be functions of dimensionless distance and the flame speed, V_f:

$$P^* = \min(P_1^*, P_2^*) , \tag{15}$$

$$I^* = \min(I_1^*, I_2^*) , \tag{16}$$

$$P_1^* = 0.34/(R^*)^{4/3} + 0.062/(R^*)^2 + 0.0033/(R^*)^3 , \tag{17}$$

$$I_1^* = 0.0353/(R^*)^{0.968} , \tag{18}$$

$$P_2^* = \frac{V_f^2}{c_0^2}\frac{\sigma-1}{\sigma}(0.83/R^* - 0.14/(R^*)^2) , \tag{19}$$

$$I_2^* = \frac{V_f}{c_0}\frac{\sigma-1}{\sigma}\left(1 - 0.4\frac{V_f}{c_0}\frac{\sigma-1}{\sigma}\right)(0.06/R^* + 0.04/(R^*)^2 - 0.0025/(R^*)^3) . \tag{20}$$

Equations (17 – 20) are presented with coefficients applicable for air explosions. These equations can be applied for ground explosions as well by using double explosion energy in (12, 14). The above description of the air blast parameters are valid for the range of dimensionless distances $0.21 < R^* < 3.77$, and for visible flame speeds $V_f \le 500$ m/s. For higher flame speeds, formulas for gas detonations (17, 18) may be used directly.

Although experimental data for hydrogen were not used in [2] to derive the above descriptions for blast parameters, the experimental results [9] reported in [10] appeared to be in a good agreement with the method presented here. This provides an additional support for application of the blast curves from [2] for the cases of hydrogen deflagrations.

2.4 Blast damage criteria

An assessment of damage potential is made here using pressure-impulse (P, I) damage criteria:

$$(I - I_a)(P - P_a) \ge k , \tag{21}$$

where I_a, P_a, and k are parameters characterising levels of equal damage. The values of parameters I_a, P_a, and k characterising different levels of damages from an air blast are collected in Table 1 [1, 11]. As suggested in [1] these (P, I) diagrams are applicable for houses, and light-frame industrial buildings (factories, main offices, and main engineering workshops). These diagrams form the basis for evaluation of safety distances adopted in the UK.

Table 1. Parameters of (P, I) diagrams for selected levels of damages.

Damage description	P_a, Pa	I_a, Pa·s	k, Pa²·s
Total destruction of buildings	70100	770	866100
Threshold for partial destruction; 50 to 75% of walls destroyed	34500	520	541000
Threshold for serious structural damage; some load bearing members fall	14600	300	119200
Border of minor structural damage	3600	100	8950

3. RESULTS AND DISCUSSION

The methodology described in the previous section is applied here to calculate standoff distances from the blast epicenter at selected levels of damages. The main variable in the calculations is the total mass of hydrogen released. The methodology is applied to three hypothetical cases of obstacles surrounding the release location:

A. High congestion. Characteristic distance between obstacles, $x = 0.2$ m; characteristic size of obstacles, $y = 0.1$ m. This situation may be typical for a unit with multiple tubes and pipelines.

B. Medium congestion. Characteristic distance between obstacles, $x = 1$ m; characteristic size of obstacles, $y = 0.5$ m. This situation may be typical for a technological unit surrounded by other units / boxes.

C. Low congestion. Characteristic distance between obstacles, $x = 4$ m; characteristic size of obstacles, $y = 2$ m. This situation may be typical for a large technological unit surrounded by other large units (e. g., refueling station)

Figure 4 shows the maximum flame speed in the hemispherical cloud as a function of the total mass of hydrogen released. It is seen that the obstacle geometry affects significantly the maximum flame speed. It would be necessary, e.g., to release 1 kg, 40 kg, and 1000 kg of H_2 in high, medium, and low congestion correspondingly to achieve the flame speed of 300 m/s.
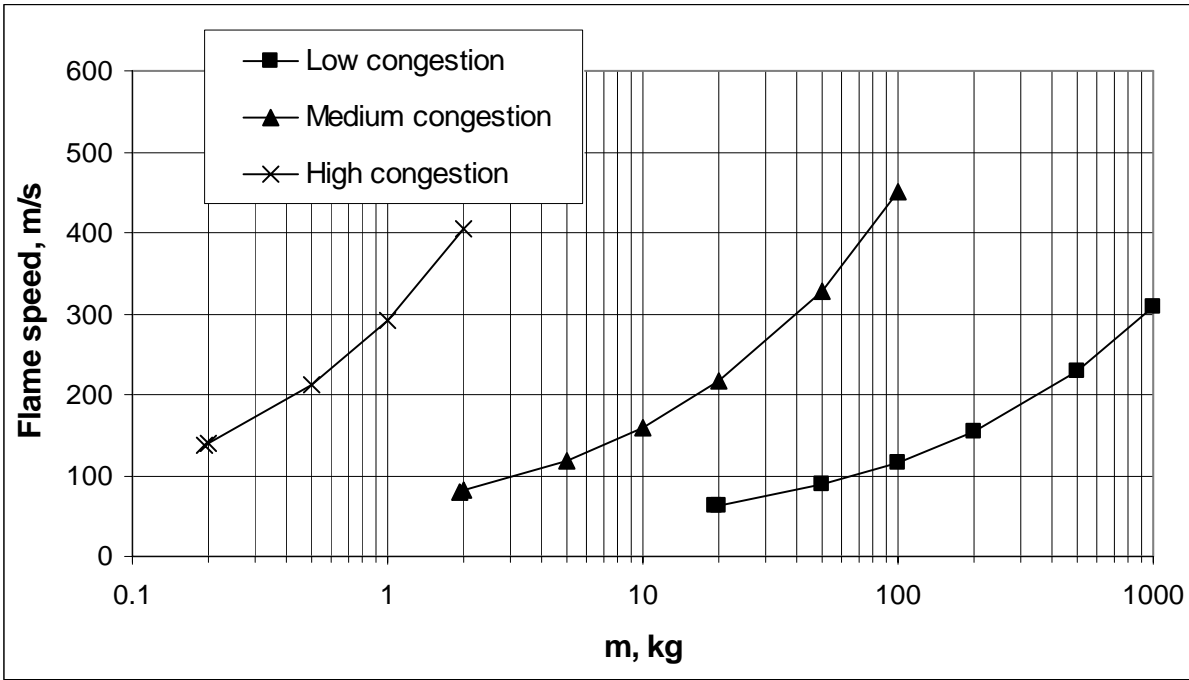

Figure 4. Flame speed in hydrogen cloud as a function of total mass of hydrogen released.

Radii from the blast epicenter to locations where selected levels of building damages can be observed versus total mass of hydrogen released for the three levels of congestion are presented in Figs. 5, 6, and 7. It is seen that a release of 10 kg of hydrogen, e.g., would not result in building damages for the case of the low congestion. The same release in the medium congestion case would result in building damages at distances of up to 40 m. In the case of the high congestion the same release would be very severe, potentially resulting in building damages at distances of up to 70 m.
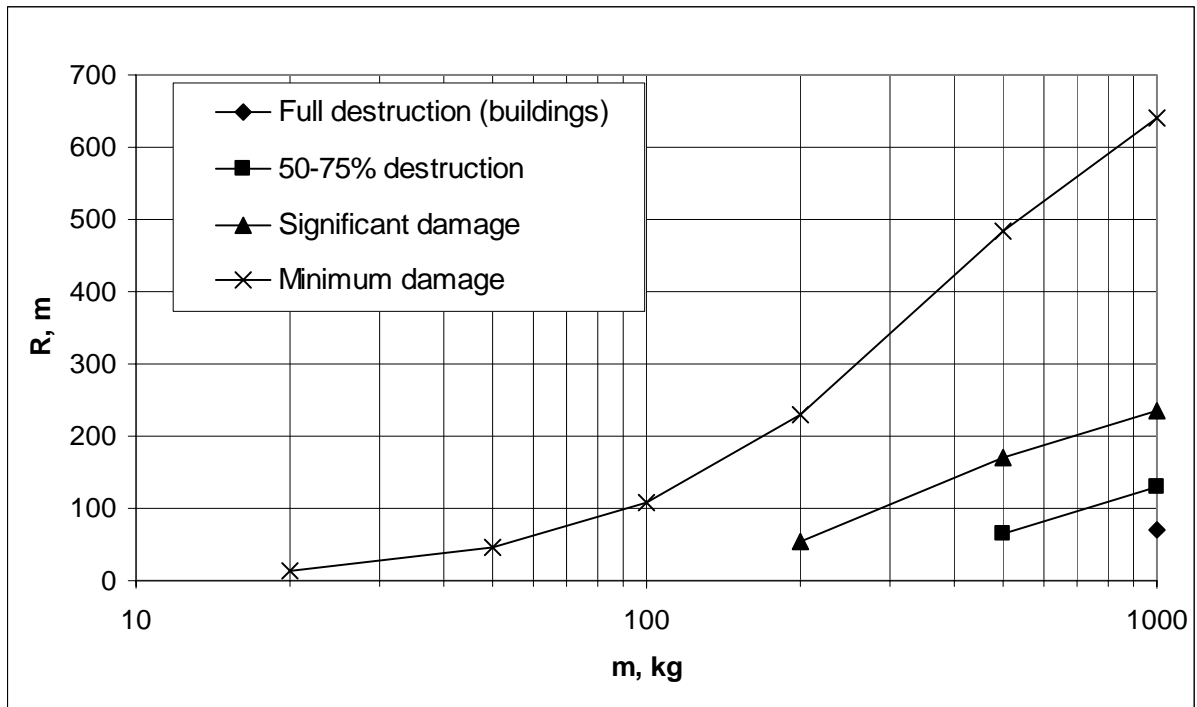
8

Figure 5. Radii from blast epicentre to locations with selected levels of building damages versus total mass of hydrogen released for low congestion.
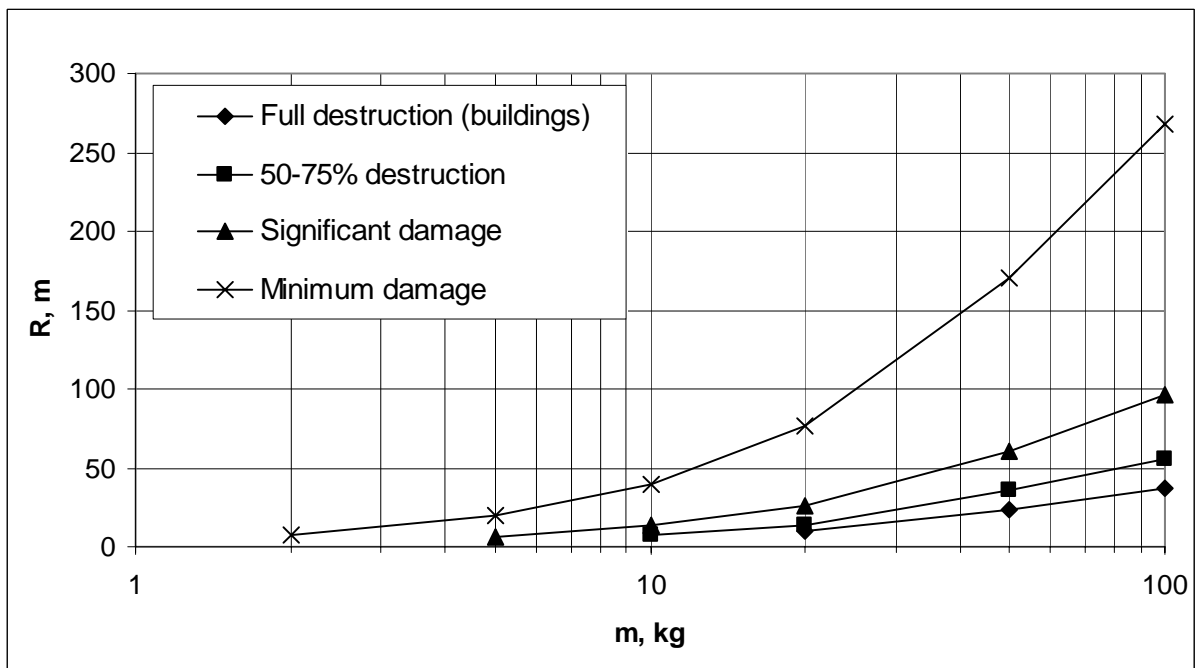

Figure 6. Radii from blast epicentre to locations with selected levels of building damages versus total mass of hydrogen released for medium congestion.
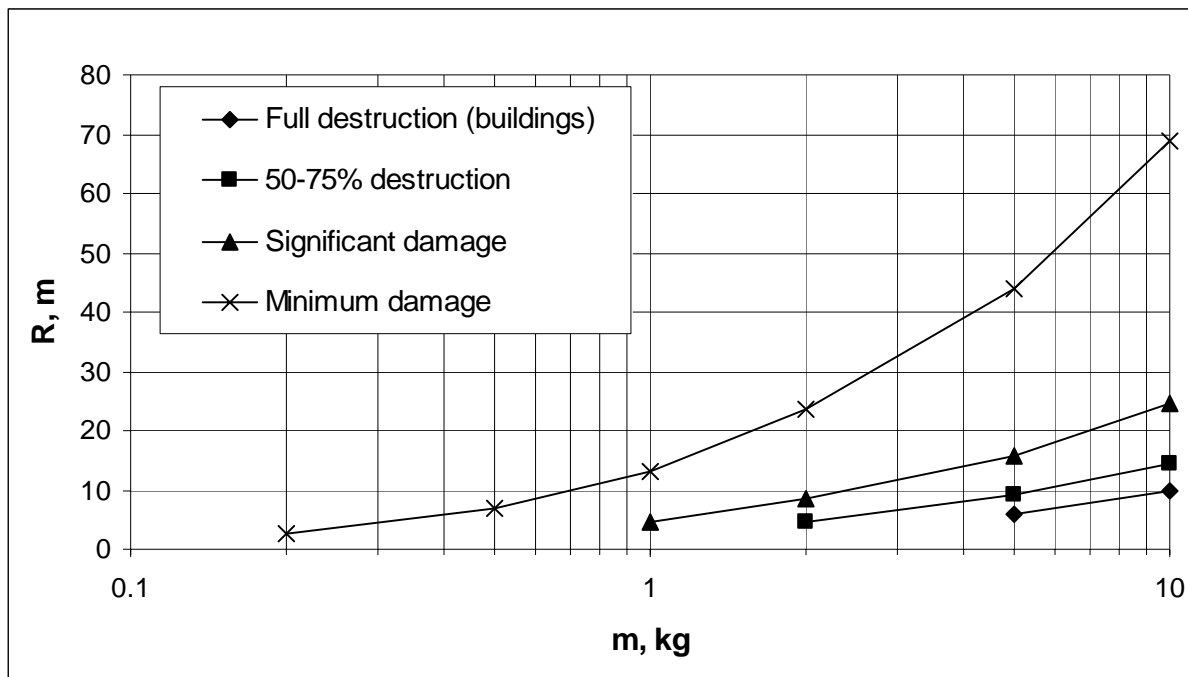
Figure 7. Radii from blast epicentre to locations with selected levels of building damages versus total mass of hydrogen released for high congestion.

The minimum building damage criterion may be used as an option for defining safety distances. It should be noted that this is not the only choice and different criteria defining safety distances may be selected. This may depend on the type of the technological unit, the type of surrounding, and/or on the applicable standards and regulations. The choice of the minimum building damage may be reasonable in many practical cases, however, it is used here as an illustration.

Figure 8 shows the safety distances (defined by the minimum damage for buildings) versus total mass of hydrogen released for the selected levels of congestion. It is seen that there are certain threshold values of the mass of hydrogen released for each level of congestion that may be considered as potentially damaging. These threshold values may be used as the target values to be achieved by safety systems designed to limit the release amount. It is seen also that for very large quantities of hydrogen released, the level of congestion becomes unimportant. Releases of about 1000 kg of hydrogen would certainly be very dangerous for any obstacle geometries.

Figure 8 also shows the curve for an ideal explosion (TNT explosion is used as an ideal source) with the energy equal to the total chemical energy of hydrogen released. This curve gives the upper bound for the safety distances based on the total energy content. It is seen that the methodology presented here suggests the safety distances that are significantly smaller than the absolute maximum values. The difference is up to an order of magnitude for the masses of hydrogen released above the threshold values for each level of congestion.

If one defines an explosion yield as a fraction of the energy of TNT-explosion that produces the same damage at a specified distance, such an energy yield for unconfined hydrogen explosions considered here varies from about 2% to 50% depending on the congestion level and mass of hydrogen released (for the masses of hydrogen released above the threshold values). This suggests that the methodology presented here is able to give more accurate estimates for safety distances compared to those based on the average explosion yield, or "TNT-equivalency" values.
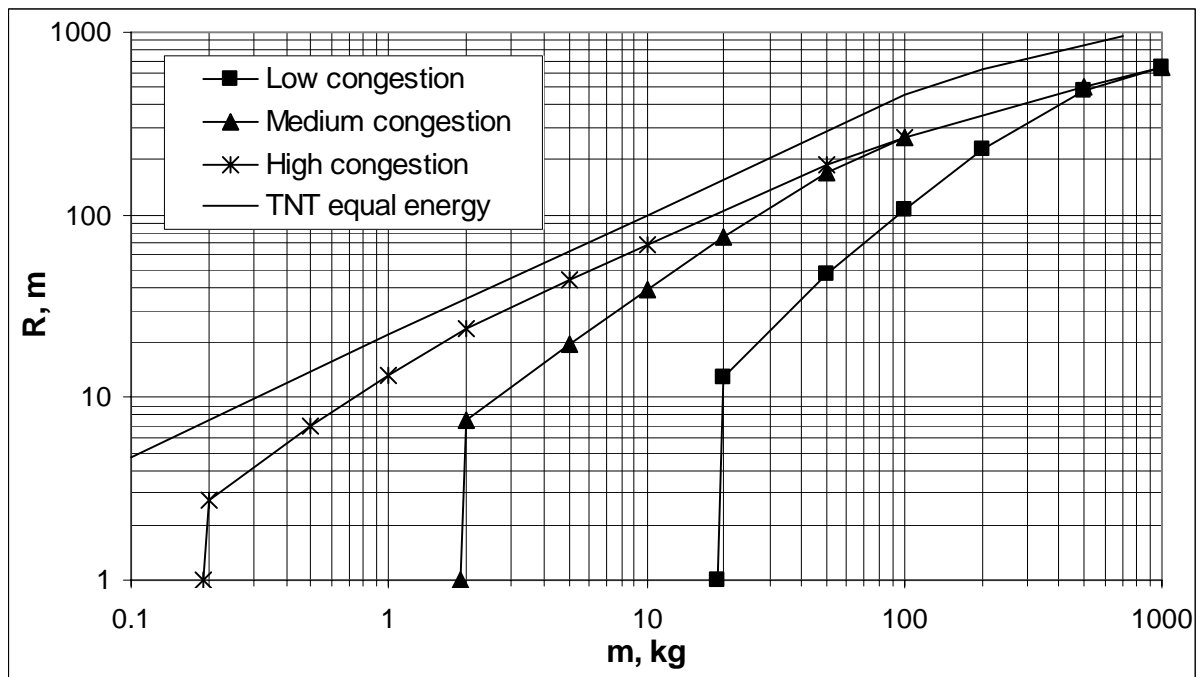
Figure 8. Safety distances (defined by minimum damage for buildings) versus total mass of hydrogen released for three selected levels of congestion.

It should be noted here that the data presented in Fig. 8 are calculated for the purpose to illustrate the methodology proposed. They cannot be used directly as safety distances for a particular hydrogen application. Each application would require a set of calculations to be performed with account for specific density of congestion and damage criteria to be used in the definition of the safety distances.

It should be also noted that the total mass of hydrogen released is not the same as the total mass of hydrogen stored on the site. Most of applications include special safety measures designed to limit the amount of hydrogen released. It is important to mention once again here that the model for hydrogen distribution and the respective "worst case" scenario is applicable to nearly instantaneous releases of hydrogen. It is very probable that relatively weak hydrogen releases would not be capable of creating the combustible mixture under unconfined conditions.

4. CONCLUSIONS

A simple approximate method for evaluation of blast effects and safety distances for unconfined hydrogen explosions has been presented. The proposed method includes: (i) a model for evaluation of the flame speeds depending on the cloud size, composition, and obstacle geometry; (ii) a model for average properties of "worst case" hydrogen distribution for cases of relatively fast hydrogen releases; (iii) a model for evaluation of air blast parameters; and (iv) a selection of blast damage criteria.

This set of models may be used as a simple approximate analytical tool for evaluation of the blast effects and safety distances for unconfined hydrogen explosions. It can be also applied as a screening tool to select the cases where a detailed analysis may be necessary.

In accordance with available observations the method predicts that the blast effect of unconfined hydrogen explosions strongly depends on the level of congestion.

It was shown that certain threshold values of the mass of hydrogen released may be defined as potentially damaging. This minimum of the mass of hydrogen released varies by several orders of

magnitude depending on the level of congestion. It was also shown that large hydrogen releases, of the order of 1000 kg, and more, become less sensitive to the obstacle geometry and can be dangerous for any level of congestion.

REFERENCES

1. Baker, W. E., P. A. Cox, P. S. Westine, J. J. Kulesz, R. A. Strehlow, Explosion Hazards and Evaluation, 1983, Elsevier, Amsterdam-Oxford-New York.
2. Dorofeev, S. B., Blast effect of confined and unconfined explosions, Shock Waves, Proceedings of the 20th ISSW, B Sturtevant, J Shepherd, H Hornung Eds., Vol. 1, pp. 77-86, 1996, Scientific Publishing Co., Singapore.
3. A. Veser, W. Breitung, S. B. Dorofeev, Run-up distances to supersonic flames in obstacle-laden tubes, *J. Phys. IV France*, **12**, No 7, 2002., pp333-340.
4. J. Grune, A. Veser, G. Stern, W. Breitung, S. Dorofeev. Acceleration of unconfined flames in congested areas. Proceedings of 19th Internat. Colloquium on the Dynamics of Explosions and Reactive Systems (ICDERS), Hakone, Japan, July 27 – August 1, 2003.
5. Bradley, D., Lau, K.C., & Lawes, M. (1992) Flame Stretch Rate as a Determinant of Turbulent Burning Velocity. *Proc. R. Soc.*, London **A338**, 359-387.
6. Pierorazio, A. P., Thomas, J. K., Baker, Q. A., Ketchum, D. E., An Update to the Baker-Strehlow-Tang Vapor Cloud Explosion Prediction Methodology Flame Speed Table, *Process Safety Progress*, **24**, No 1, 2005, pp 59-65.
7. Groethe, M., Colton, J., Choba, S., Sato, Y., Hydrogen Deflagrations at Large Scale, Proceedings of the World Hydrogen Energy Conference, Japan, 2004.
8. Geisbrecht, H., Hess, K., Leuckel W., Maurer, B., Analysis of Explosion Hazards on Spontaneous Release of Inflammable Gases into the Atmosphere, *Ger. Chem. Eng.* **4**, 1981, pp 305-314.
9. Schneider, H. and Pförtner, H., PNP-Sichcrheitssofortprogramm, Prozebgasfreisetzung-Explosion in der Gasfabrik und Auswirkungen von Druckwellen auf das Containment. Dezember 1983, Fraunhofer-ICT internal report.
10. Molkov, V.V., Makarov, D.V. and Schneider, H., Hydrogen-Air Deflagrations in Open Atmosphere: Large Eddy Simulation Analysis of Experimental Data. Proceedings of 1st International Conference on Hydrogen Safety, Pisa, September 8-10, 2005.
11. Jarrett, D. E., Derivation of British Explosive Safety Distances, *Annals of the New York Academy of Sciences*, **152**, 1968, Article 1, pp 18 –35.